OPEN ACCESS

Semifluxons in superconductivity and cold atomic gases

New Journal of Physics
The open-access journal for physics

Semifluxons in superconductivity and cold atomic gases

R Walser[1,3], E Goldobin[2], O Crasser[1], D Koelle[2], R Kleiner[2] and W P Schleich[1]

[1] Institut für Quantenphysik, Universität Ulm, Albert-Einstein Allee 11, D-89069 Ulm, Germany
[2] Physikalisches Institut II, Universität Tübingen, Auf der Morgenstelle 14, D-72076 Tübingen, Germany
E-mail: Reinhold.Walser@uni-ulm.de

New Journal of Physics **10** (2008) 045020 (16pp)
Received 21 December 2007
Published 30 April 2008
Online at http://www.njp.org/
doi:10.1088/1367-2630/10/4/045020

Abstract. Josephson junctions (JJs) and junction arrays are well-studied devices in superconductivity. With external magnetic fields one can modulate the phase in a long junction and create traveling, solitonic waves of magnetic flux, called fluxons. Today, it is also possible to devise two different types of junctions: depending on the sign of the critical current density $j_c \gtrless 0$, they are called 0- or π-junctions. In turn, a 0–π junction is formed by joining two of these junctions. As a result, one obtains a pinned Josephson vortex of fractional magnetic flux, at the 0–π boundary. Here, we analyze this arrangement of superconducting junctions in the context of an atomic bosonic quantum gas, where two-state atoms in a double well trap are coupled in an analogous fashion. There, an all-optical 0–π JJ is created by the phase of a complex valued Rabi frequency and we derive a discrete four-mode model for this situation, which qualitatively resembles a semifluxon.

[3] Author to whom any correspondence should be addressed.

Contents

1. Introduction

During the past two decades, the field of cold atomic gases has come a long way starting from almost lossless trapping and cooling techniques [1] to reaching quantum degeneracy of bosons and fermions [2]. Many phenomena that are the hallmarks of condensed matter physics, whether in superfluid or superconducting materials [3], are revisited within this novel context. Due to the remarkable ease with which it is possible to isolate the key mechanisms from rogue processes, one can clearly identify phase transitions, for example, Bose–Einstein condensation (BEC), the Mott phase transition or the BEC–BCS crossover. Today however, degenerate gases are still at a disadvantage if we consider robustness, portability or the ability for mass production compared to solid-state devices, which is a great achievement of the semiconductor industry. Strong attempts to miniaturize cold gas experiments ([4]; [5] and references therein) and to make them portable [6]–[9] are currently under way in many laboratories.

Due to the great importance and practical relevance of the Josephson effect to superconducting systems [10]–[12], it also received immediate attention after the first realization of BECs [13]–[26] and superfluid atomic fermions [27], more recently. In particular, the combination of optical lattices with ultracold gases [28, 29] has boosted the possibilities of investigating junction arrays experimentally. Remarkably, even the absence of phase-coherence between neighboring sites can lead to interference as demonstrated in [30]. The possibility of studying atomic Josephson vortices in the mean field description was raised first in connection with the sine-Gordon equation [31, 32].

In the present paper, we will report on such a transfer of concepts from a superconducting device [33], i.e. in various realizations of Josephson junction (JJ) arrays and their unusual state properties of traveling (fluxons) and pinned (semifluxons) magnetic flux quanta, to an analogous set-up for neutral bosonic atoms in a trap. In particular, we will investigate an all-optical 0–π JJ that can be created with a jumping phase of an optical laser.

This paper is organized as follows: in section 2, we give a brief review of the current status of the superconductor physics of JJs. In particular, we refer to the most relevant publications in this thriving field of fluxon and semifluxon physics; in section 3, we discuss a similar set-up, which allows us to find a pinned semifluxon in an atomic 0–π JJ and we compare the results. Finally, we discuss further open questions in section 4.

2. Fluxons and semifluxons in superconductivity

The Josephson effect is a well-established phenomenon in solid-state physics. A JJ consists of two weakly coupled superconducting condensates. JJs are usually fabricated artificially using low- or high-T_c superconducting electrodes separated by a thin insulating (tunnel), normal metal, or some other (exotic) barrier. JJs can also be present intrinsically in an anisotropic layered high-T_c superconductor such as $Bi_2Sr_2Ca_1Cu_2O_8$ [34, 35].

The dc Josephson effect (flow of current through a JJ without producing a voltage drop, i.e. without dissipation) is expressed using the first Josephson relation, which in the simplest case has the form

$$I_s = I_c \sin(\phi), \tag{1}$$

where I_s is the supercurrent flowing through the junction, I_c is the critical current, i.e. the maximum supercurrent which can pass through the JJ, and $\phi = \theta_2 - \theta_1$ is the difference between the phases of the quantum mechanical macroscopic wavefunctions $\psi_{1,2} = \sqrt{n_s}e^{i\theta_{1,2}}$ of the superconducting condensates in the electrodes.

Recent advances in physics and technology allow the fabrication and study of the so-called π-JJs—junctions which formally have negative critical current $I_c < 0$. This can be achieved by using a ferromagnetic barrier, i.e. in superconductor–ferromagnet–superconductor (SFS) [36]–[40] or superconductor–insulator–ferromagnet–superconductor (SIFS) [41, 42] structures. One can also achieve the same effect using a barrier which effectively flips the spin of a tunneling electron, e.g. when the barrier is made of a ferromagnetic insulator [43], of a carbon nanotube [44] or of a quantum dot created by gating a semiconducting nanowire [45].

The change in the sign of a critical current has far-reaching consequences. For example, analyze the Josephson energy (potential energy related to the supercurrent flow). In a conventional JJ with $I_c > 0$,

$$U(\phi) = E_J(1 - \cos\phi) \tag{2}$$

and has a minimum at $\phi = 0 + 2\pi n$ (the ground state), where $E_J = \Phi_0 I_c/2\pi$ is the Josephson energy. If $I_c < 0$, we define $E_J = \Phi_0|I_c|/2\pi > 0$ and

$$U(\phi) = E_J(1 + \cos\phi). \tag{3}$$

Obviously, the minimum of energy is reached for $\phi = \pi + 2\pi n$. Thus, in the ground state (the JJ is not connected to a current source, no current flows through it), the phase drop across a conventional JJ with $I_c > 0$ is $\phi = 0 + 2\pi n$, while for a junction with $I_c < 0$ it is $\phi = \pi + 2\pi n$. Therefore, one speaks about '0-JJs' and 'π-JJs'.

Further, connecting the two superconducting electrodes of a π-JJ by a not very small inductor L (superconducting wire), the supercurrent $\propto \pi/L$ will start circulating in the loop. Note that this supercurrent is spontaneous, i.e. it appears by itself, and has a direction randomly chosen between clockwise and counterclockwise [46]. The magnetic flux created by this supercurrent inside the loop is equal to $\Phi_0/2$, where $\Phi_0 = h/2e \approx 2.07 \times 10^{-15}$ Wb is the magnetic flux quantum. Thus, the π-JJ works as a *phase battery*. This phase battery will work as described, supplying a supercurrent through the loop with the inductor, provided the inductance $L \gg \Phi_0/I_c$. If the inductance L is not that large, the battery will be overloaded, providing a smaller phase drop and supporting smaller current. For very small inductance the battery will stop working completely.

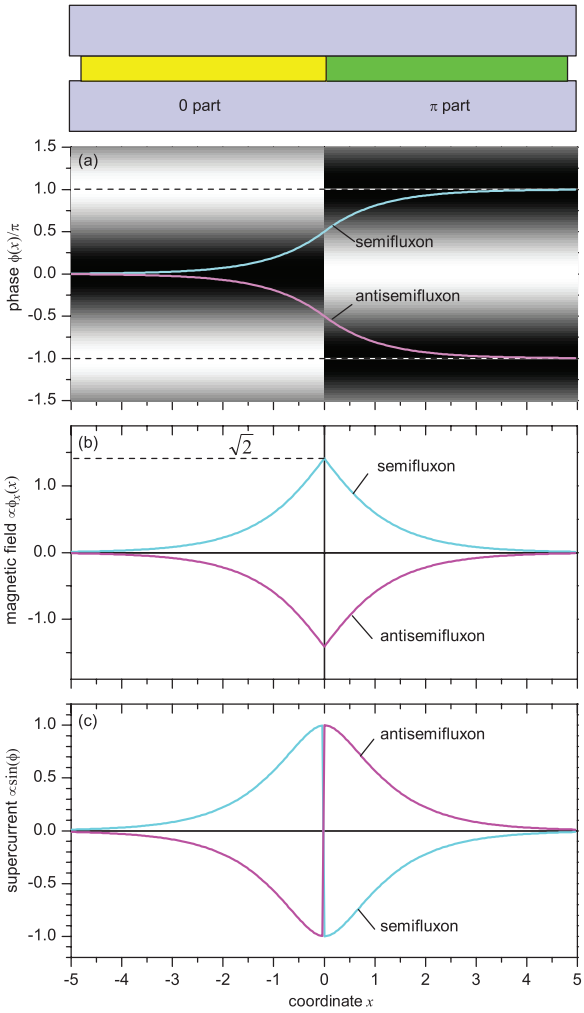

Figure 1. Sketch of a 0–π JJ and profiles of (a) the phase $\phi(x)$, (b) the magnetic field $\propto \mathrm{d}\phi(x)/\mathrm{d}x$ and (c) the supercurrent density $j_\mathrm{s}(x) \propto \sin\phi(x)$ corresponding to a semifluxon (blue/light gray) and antisemifluxon (pink/dark gray). The gray shading in subplot (a) represents the Josephson (potential) energies of equations (2) and (3), where dark is low and light means high values.

Similar effects can be observed in a π dc superconducting quantum interference device (SQUID; one 0-JJ, one π-JJ and an inductor L connected in series and closed in a loop) or in 0–π JJ. Let us focus on the latter case.

Consider a long (along x) Josephson junction (LJJ) one half of which at $x < 0$ has the properties of a 0-JJ (critical current *density* $j_\mathrm{c} > 0$) and the other half at $x > 0$ has the properties of a π-JJ (critical current *density* $j_\mathrm{c} < 0$). Long means that the length is much larger than the so-called Josephson length λ_J, which characterizes the size of a Josephson vortex; typically $\lambda_\mathrm{J} \sim 10$–$20\ \mu$m. What will be the ground state of such a 0–π LJJ? It turns out that if the junction is long enough (formally infinitely long), then far away from the 0–π boundary situated at $x = 0$, i.e. at $x \to \pm\infty$, the phase ϕ will have the values 0 or $\pm\pi$ (we omit $2\pi n$ here), while in the vicinity of the 0–π boundary the phase $\phi(x)$ smoothly changes from $\phi(-\infty) = 0$ to $\phi(+\infty) = \pm\pi$, see figure 1(a). The exact profile can be derived analytically [33, 47, 48]. Since

the phase bends, the local magnetic field $H \propto \mathrm{d}\phi/\mathrm{d}x$ will be localized in the vicinity of the 0–π boundary and carry the total flux equal to $\pm\Phi_0/2$, see figure 1(b). The sign depends on whether the phase bends from $\phi(-\infty) = 0$ to $\phi(+\infty) = +\pi$ or to $\phi(+\infty) = -\pi$. Thus, such an object is called a semifluxon or an antisemifluxon. If one analyzes the Josephson supercurrent density flowing though the barrier $j_s(x) = j_c(x)\sin\phi(x)$, one can see in figure 1(c) that the supercurrent has different directions on different sides of the 0–π boundary. Since we do not apply any external current, the flow of current should close in the top and bottom electrodes, i.e. the supercurrent circulates (counter)clockwise in the case of (anti)semifluxon. Thus, *a semifluxon is a Josephson vortex of supercurrent. It is pinned at the* 0–π *boundary and has two degenerate ground states with the localized magnetic field carrying the flux* $\pm\Phi_0/2$.

Semifluxons in various types of JJs have been actively investigated during the last few years. In fact, the first experiments became possible because of a deeper understanding of the symmetry of the superconducting order parameter in cuprate superconductors. This order parameter with so-called d-wave symmetry is realized in anisotropic superconductors, such as $YBa_2Cu_3O_7$ or $Nd_{2-x}Ce_xCuO_4$. It allowed the fabrication of 0–π grain boundary LJJs [49, 50] and, later, more controllable d-wave/s-wave ramp zigzag JJs [51, 52] and the ability to directly see and manipulate semifluxons using a SQUID microscope [53, 54].

Semifluxons are very interesting nonlinear objects: they can form a variety of ground states [55]–[58], may flip [49, 53] emitting a fluxon [57, 59, 60], or be rearranged [61] by a bias current. Huge arrays of semifluxons were realized [53] and predicted to behave as tunable photonic crystals [62]. Semifluxons are also promising candidates for storage devices in the classical or quantum domain and can be used to build qubits [63] as they behave like macroscopic spin 1/2 particles.

Now, an interesting question arises: can one realize π or even 0–π JJs in an atomic BEC? In the latter case, the degenerate ground state corresponding to a semifluxon should have a nontrivial spatial phase profile and semifluxon physics can also be studied using BEC implementation.

3. Semifluxons in BECs

Here, we will address this question and examine a configuration where the two-state atoms are trapped in a quasi-one-dimensional (1D) cigar-shaped trap with an additional superimposed double-well potential in the longitudinal direction. The spatial localization of the two-state atoms inside the double-well potential leads to two internal atomic JJs that are driven via an optical, complex valued '0–π' laser field and they are motionally connected via tunneling.

First, we will present details of the model and introduce the Hamiltonian of the system. Then, we will examine the classical limit of the field theory and study the ground state of the Gross–Pitaevskii equation. Finally, we will exploit the fact that the spatial wavefunctions are localized inside a deep double well and study a simple four-mode quantum model derived from a Wannier basis state representation.

3.1. 0–π*-junction in a BEC*

To model the 0–π-junction [31, 32] in a BEC, we are guided by the condensed matter physics set-up depicted in figure 2 and replace the two superconductors by an atomic two-level BEC in a cigar-shaped trap. The two states of the atom, i.e. the excited state $|e\rangle$ and ground state

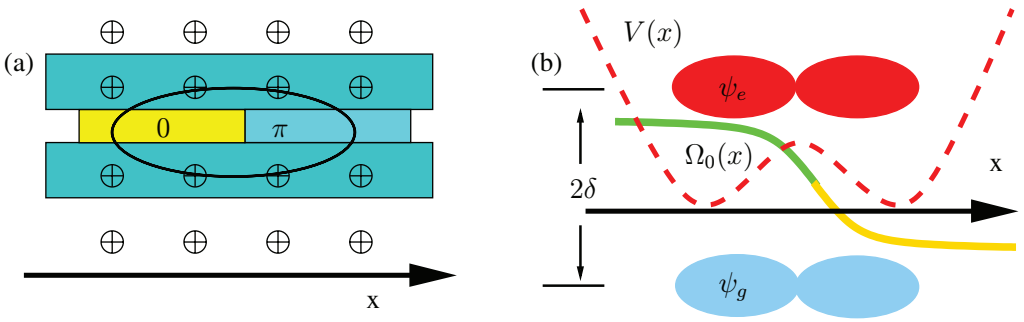

Figure 2. Analogy of a 0–π JJ in a superconductor (a) with an atomic two-level BEC (b) in a double well trap $V(x)$ with a position dependent Rabi frequency $\Omega_0(x)$. The excited atomic level $|e\rangle$ is separated from the ground level $|g\rangle$ by the detuning 2δ.

$|g\rangle$, couple via a position-dependent Rabi frequency $\Omega_0(x)$, which exhibits a phase jump at the origin of the x-axes

$$\Omega_0(x) = \begin{cases} \Omega_0, & x < 0, \\ \Omega_1 = -\Omega_0, & x \geqslant 0. \end{cases} \tag{4}$$

In this quasi-1D scenario, we will represent the two-state atoms by a spinorial bosonic quantum field $\hat{\Psi}$, which satisfies the commutator relation

$$[\hat{\Psi}(x), \hat{\Psi}^\dagger(y)] = \mathbb{1}\delta(x-y). \tag{5}$$

This field can be decomposed in any complete single particle basis $|\sigma, l\rangle$, which resolves the spatial extent of the field and the internal structure of the atoms, i.e.

$$\hat{\Psi} = \sum_{\sigma=\{e,g\}} \sum_{l=0}^{\infty} |\sigma, l\rangle\, \hat{a}_{\sigma,l} \tag{6}$$

and we denote the corresponding discrete bosonic field amplitudes by $\hat{a}_{\sigma,l}$. Here, σ characterizes the internal states by (e, g) and the external motion in the double-well potential by a quantum label l. The dynamical evolution of the atomic field is governed by the following Hamiltonian:

$$\begin{aligned} \hat{H} = \int_{-\infty}^{\infty} \mathrm{d}x\, \hat{\Psi}^\dagger(x) \left[-\partial_x^2 + V(x) + \begin{pmatrix} \delta & \Omega_0(x) \\ \Omega_0^*(x) & -\delta \end{pmatrix} \right] \hat{\Psi}(x) \\ + g\hat{\Psi}_e^\dagger(x)\hat{\Psi}_e^\dagger(x)\hat{\Psi}_e(x)\hat{\Psi}_e(x) + g\hat{\Psi}_g^\dagger(x)\hat{\Psi}_g^\dagger(x)\hat{\Psi}_g(x)\hat{\Psi}_g(x). \end{aligned} \tag{7}$$

Here, we use dimensionless units, in particular we have set $\hbar = 1$ and the mass of the atom $m = 1$. The energy consists of the single particle energy in a trap $V(x)$, which is identical for both species, the electric dipole interaction of the two-state atom [64], as well as a generic collision energy proportional to the coupling constant $g = g_{ee} = g_{gg}$. To simplify the analysis, we have deliberately set the cross-component scattering length $g_{eg} = 0$. No unaccounted loss channels are present. Therefore, we have number conservation

$$[\hat{H}, \hat{N}] = 0, \tag{8}$$

as a symmetry. If we denote a generic state of the many-particle system in Fock space by

$$|\psi(t)\rangle = \sum_{\mathbf{n}=0}^{\infty} \psi_{\mathbf{n}}(t)|\mathbf{n} = (n_0, n_1, \ldots)\rangle, \tag{9}$$

then one can obtain the dynamics of the system most generally from the Lagrangian formulation

$$\mathcal{L}[\psi_{\mathbf{n}}(t), \dot{\psi}_{\mathbf{n}}(t)] = \langle\psi(t)|\mathrm{i}\partial_t - \hat{H}|\psi(t)\rangle. \tag{10}$$

In field theory, the canonical momentum is given by $\pi_{\mathbf{n}} = \delta\mathcal{L}/\delta\dot{\psi}_{\mathbf{n}} = \mathrm{i}\psi^*_{\mathbf{n}}$. From the Hamilton equation $\dot{\pi}_{\mathbf{n}} = \delta\mathcal{L}/\delta\psi_{\mathbf{n}}$, one recovers the conventional Schrödinger equation in Fock space

$$\mathrm{i}\partial_t|\psi\rangle = \hat{H}|\psi\rangle. \tag{11}$$

The Lagrangian approach is obviously a central concept in the path integral formulation of quantum mechanics [65]. However, it is also of great utility in the approximate description of the dynamics if we connect it with concepts of classical mechanics as we will see in the following.

3.2. Spatially extended classical model: the Gross–Pitaevskii equation

The classical limit of the field equations [2] can be recovered quickly by approximating the state of the system by a coherent state

$$\hat{\Psi}_\sigma(x)|\psi\rangle = \psi_\sigma(x)|\psi\rangle. \tag{12}$$

Within this approximation, we obtain from the Lagrangian of equation (10) the two-component Gross–Pitaevskii equation $\psi = (\psi_e(x,t), \psi_g(x,t))^\top$

$$\mathrm{i}\partial_t\psi = \left[-\partial_x^2 + V(x) + \begin{pmatrix} \delta + 2g|\psi_e|^2 & \Omega_0(x) \\ \Omega_0^*(x) & -\delta + 2g|\psi_g|^2 \end{pmatrix}\right]\psi. \tag{13}$$

For a macroscopically occupied field this equation models the spatial evolution of the coupled JJs very well [17]–[21], [23]–[25], [32].

3.3. Discrete quantum model: two coupled JJs

To gain more insight into the quantum properties of the ground state of the system [63], one can decompose the atomic field into its principal components and disregard small corrections. Recently, the use of Wannier basis states [66] was popularized in a seminal article of Jaksch *et al* [67] to derive a Bose–Hubbard model for atoms in optical lattices.

In our situation, we want to consider a double-well potential as the limiting case of a periodic lattice. While even and odd parity modes relate to delocalized Bloch states in a periodic system, left and right localized modes, i.e. φ_0 and right φ_1, resemble the Wannier basis. No particular emphasis is given to the shape of the double-well potential. Therefore, we simply construct even and odd parity Bloch states from displaced Gaussians. By a further orthogonal transformation, we have obtained the localized Wannier modes, which are depicted in figure 3. With respect to these basis states, we can approximate the field with four modes

$$\hat{\Psi}_e(x) = \hat{e}_0\varphi_0(x) + \hat{e}_1\varphi_1(x) + \delta\hat{\Psi}_e, \tag{14}$$

$$\hat{\Psi}_g(x) = \hat{g}_0\varphi_0(x) + \hat{g}_1\varphi_1(x) + \delta\hat{\Psi}_g. \tag{15}$$

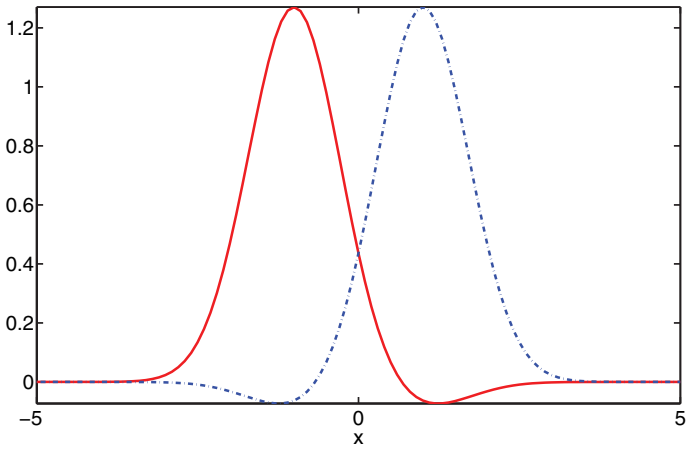

Figure 3. From even and odd parity modes of a double-well potential, one can construct the left φ_0 (solid line) and right φ_1 (dashed-dotted line) localized Wannier states of the system.

The four bosonic amplitudes $\{\hat{g}_0, \hat{e}_0, \hat{g}_1, \hat{e}_1\}$ satisfy the usual commutation relations and we will disregard the small corrections of order $\delta\hat{\Psi}_\sigma$.

If this approximate field is substituted in the Hamiltonian, equation (7), we can exploit the orthogonality of the wavefunctions and obtain the two-body matrix elements φ_{ijkl}

$$\delta_{ij} = \int_{-\infty}^{\infty} \mathrm{d}x\, \varphi_i(x)\varphi_j(x), \qquad \varphi_{ijkl} = \int_{-\infty}^{\infty} \mathrm{d}x\, \varphi_i(x)\varphi_j(x)\varphi_k(x)\varphi_l(x). \tag{16}$$

Out of the 16 combinations for φ_{ijkl}, we only retain the physically most relevant contributions and disregard others deliberately. This leads to the following model Hamiltonian for two coupled JJs:

$$\begin{aligned}\hat{H} = {} & \Lambda(\hat{e}_0^\dagger\hat{e}_1 + \hat{e}_1^\dagger\hat{e}_0 + \hat{g}_0^\dagger\hat{g}_1 + \hat{g}_1^\dagger\hat{g}_0) + \delta(\hat{e}_0^\dagger\hat{e}_0 - \hat{g}_0^\dagger\hat{g}_0) + \delta(\hat{e}_1^\dagger\hat{e}_1 - \hat{g}_1^\dagger\hat{g}_1) \\ & + \Omega_0(\hat{e}_0^\dagger\hat{g}_0 + \hat{g}_0^\dagger\hat{e}_0) + \Omega_1(\hat{e}_1^\dagger\hat{g}_1 + \hat{g}_1^\dagger\hat{e}_1) + g(\hat{e}_0^\dagger\hat{e}_0^\dagger\hat{e}_0\hat{e}_0 + \hat{g}_0^\dagger\hat{g}_0^\dagger\hat{g}_0\hat{g}_0 + \hat{e}_1^\dagger\hat{e}_1^\dagger\hat{e}_1\hat{e}_1 + \hat{g}_1^\dagger\hat{g}_1^\dagger\hat{g}_1\hat{g}_1),\end{aligned} \tag{17}$$

where all coupling constants are implicitly rescaled by the corresponding single particle or two-body matrix elements and the new parameter Λ measures the spatial hopping rate between the sites.

3.4. Fock-space representation of the four-mode model

In principle, it is possible to solve the four-mode Schrödinger equation in Fock space by projecting it on the N-particle sector

$$|\psi, N\rangle = \delta(\hat{N} - N) \sum_{\mathbf{n}=0}^{\infty} \psi_{\mathbf{n}} |\mathbf{n} = (n_0^e, n_0^g, n_1^e, n_1^g)\rangle. \tag{18}$$

The number constraint on the state remains valid throughout the time evolution as number conservation is encoded into our Hamiltonian from the beginning in equation (8). This reduces the discrete $d = 4$ dimensional eigenvalue problem to an effective 3D problem with nontrivial

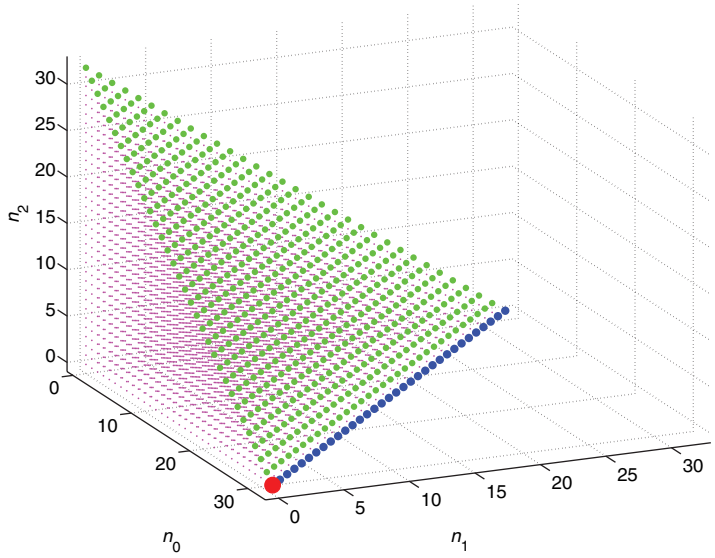

Figure 4. A 3D simplex represents the four-mode Fock space for $N = 32$ particles. The axes are labeled in a generic lexicographical order (n_0, n_1, n_2) and implicitly $n_4 = N - n_0 - n_1 - n_2$.

boundaries. We have illustrated the finite support of the amplitude field $\psi_{\mathbf{n}}$ in figure 4. It is a $(d-1)$-dimensional simplex embedded into a d-dimensional Fock space. The full analysis of this problem is an interesting problem in its own right and will be presented in a forthcoming publication.

3.5. The classical limit of the four-mode model

It is not necessary to solve the four-mode problem in Fock space to understand the principal features of the equilibrium configuration. Thus, we will again resort to the classical approximation and use the number-symmetry broken coherent state approximation for the quantum state

$$|\psi\rangle = |\boldsymbol{\alpha} = (e_0, g_0, e_1, g_1)^\top\rangle, \qquad \hat{e}_i|\psi\rangle = e_i|\psi\rangle, \qquad \hat{g}_i|\psi\rangle = g_i|\psi\rangle. \tag{19}$$

The dynamics is simply obtained from the Lagrangian

$$\mathcal{L}(\boldsymbol{\alpha}, \dot{\boldsymbol{\alpha}}) = \langle\boldsymbol{\alpha}|\mathrm{i}\partial_t - \hat{H}|\boldsymbol{\alpha}\rangle = \mathrm{i}\boldsymbol{\alpha}^*\dot{\boldsymbol{\alpha}} - \mathcal{H}(\boldsymbol{\alpha}, \boldsymbol{\alpha}^*) - \frac{\mathrm{i}}{2}\frac{\mathrm{d}}{\mathrm{d}t}\mathcal{N}(\boldsymbol{\alpha}, \boldsymbol{\alpha}^*), \tag{20}$$

if we introduce the classical Hamilton functions $\mathcal{H}(\boldsymbol{\alpha}, \boldsymbol{\alpha}^*) = \langle\boldsymbol{\alpha}|\hat{H}|\boldsymbol{\alpha}\rangle$ and number expectation values $\mathcal{N}(\boldsymbol{\alpha}, \boldsymbol{\alpha}^*) = \langle\boldsymbol{\alpha}|\hat{N}|\boldsymbol{\alpha}\rangle$ as

$$\begin{aligned}\mathcal{H}(\boldsymbol{\alpha}, \boldsymbol{\alpha}^*) = {} & \Lambda(e_0^*e_1 + e_1^*e_0 + g_0^*g_1 + g_1^*g_0) + \delta_0(|e_0|^2 - |g_0|^2) + \delta_1(|e_1|^2 - |g_1|^2) \\ & + \Omega_0(e_0^*g_0 + g_0^*e_0) + \Omega_1(e_1^*g_1 + g_1^*e_1) + g(|e_0|^4 + |g_0|^4 + |e_1|^4 + |g_1|^4),\end{aligned} \tag{21}$$

$$\mathcal{N}(\boldsymbol{\alpha}, \boldsymbol{\alpha}^*) = |e_0|^2 + |g_0|^2 + |e_1|^2 + |g_1|^2. \tag{22}$$

If the dynamical coordinate is $\boldsymbol{\alpha}$, then we find the canonical momentum as

$$\pi_k = \frac{\partial \mathcal{L}}{\partial \dot{\alpha}_k} = \mathrm{i}\alpha_k^*. \tag{23}$$

Consequently, variables and momenta obey the Poisson bracket $\{\alpha_j, \pi_k\} = \delta_{jk}$. By construction, number conservation is satisfied dynamically as

$$\frac{\mathrm{d}}{\mathrm{d}t}\mathcal{N} = \{\mathcal{H}, \mathcal{N}\} = 0 \tag{24}$$

and the Hamilton equations of motion for the coordinates read

$$\frac{\mathrm{d}}{\mathrm{d}t}\boldsymbol{\alpha} = \{\mathcal{H}, \boldsymbol{\alpha}\} = -\mathrm{i}\mathcal{K}\boldsymbol{\alpha}, \tag{25}$$

$$\mathcal{K} = \begin{pmatrix} \delta_0 + 2g|\alpha_0|^2 & \Omega_0 & \Lambda & 0 \\ \Omega_0 & -\delta_0 + 2g|\alpha_1|^2 & 0 & \Lambda \\ \Lambda & 0 & \delta_1 + 2g|\alpha_2|^2 & \Omega_1 \\ 0 & \Lambda & \Omega_1 & -\delta_1 + 2g|\alpha_3|^2 \end{pmatrix}.$$

In classical mechanics, we can deliberately choose new coordinates and momenta to account for symmetries of the Hamiltonian. If a new variable of a canonical transformation matches a conserved quantity, it follows that the conjugate variable becomes cyclic. In this spirit, we will introduce the following pairs of action-angle variables: $(\Phi, \mathcal{N})$ measures the global phase and the total particle number $\mathcal{N} = n_0^g + n_0^e + n_1^g + n_1^e$ of the system, $(\theta, \mathcal{M})$ measures the relative phase between left and right sites and the population imbalance $\mathcal{M} = n_0^e + n_0^g - (n_1^e + n_1^g)$ in between, $(\phi_0, \mathcal{M}_0 = n_0^e - n_0^g)$ and $(\phi_1, \mathcal{M}_1 = n_1^e - n_1^g)$ measure the relative internal phase of the atoms on each site and the corresponding population difference. This coupling scheme for the phases and population imbalances has been illustrated in figure 5. By inverting the population relations, one finds the individual occupation number n_l^σ per site as

$$\begin{aligned} n_0^e &= \tfrac{1}{4}(\mathcal{N} + \mathcal{M} + 2\mathcal{M}_0), \qquad & n_0^g &= \tfrac{1}{4}(\mathcal{N} + \mathcal{M} - 2\mathcal{M}_0), \\ n_1^e &= \tfrac{1}{4}(\mathcal{N} - \mathcal{M} + 2\mathcal{M}_1), \qquad & n_1^g &= \tfrac{1}{4}(\mathcal{N} - \mathcal{M} - 2\mathcal{M}_1). \end{aligned} \tag{26}$$

Finally, we can use these physical coordinates in a canonical transformation from complex amplitudes to real action-angle variables

$$\begin{aligned} e_0 &= \mathrm{e}^{-\mathrm{i}(\Phi+\theta+\phi_0)}\sqrt{n_0^e}, \qquad & g_0 &= \mathrm{e}^{-\mathrm{i}(\Phi+\theta-\phi_0)}\sqrt{n_0^g} \\ e_1 &= \mathrm{e}^{-\mathrm{i}(\Phi-\theta+\phi_1)}\sqrt{n_1^e}, \qquad & g_1 &= \mathrm{e}^{-\mathrm{i}(\Phi-\theta-\phi_1)}\sqrt{n_1^g}. \end{aligned} \tag{27}$$

For later use it is also useful to introduce the auxiliary phases θ_i, which are global phases of the subsystem on site i:

$$\theta_0 = \Phi + \theta, \qquad \theta_1 = \Phi - \theta. \tag{28}$$

By substituting field amplitudes into the Lagrangian of equation (20), one can again identify the variables and corresponding canonical momenta as

$$\frac{\partial \mathcal{L}}{\partial \dot{\Phi}} = \mathcal{N}, \qquad \frac{\partial \mathcal{L}}{\partial \dot{\theta}} = \mathcal{M}, \qquad \frac{\partial \mathcal{L}}{\partial \dot{\phi}_0} = \mathcal{M}_0, \qquad \frac{\partial \mathcal{L}}{\partial \dot{\phi}_1} = \mathcal{M}_1. \tag{29}$$

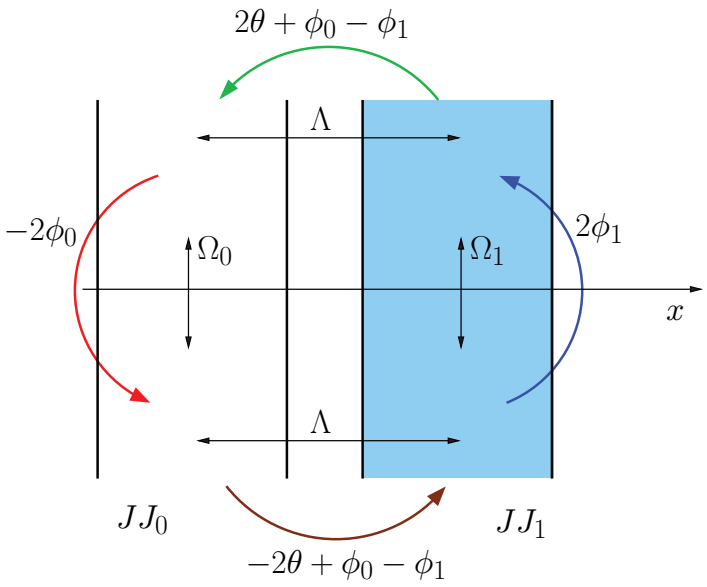

Figure 5. Coupling pattern of two coupled JJs JJ_0 and JJ_1 with local Rabi frequencies Ω_i and intersite hopping rates Λ. By definition, the sum of the phase differences vanishes, but one obtains the extra π-phase from the sign change of the Rabi coupling $\Omega_1 = -\Omega_0 = \mathrm{e}^{\mathrm{i}\pi}\Omega_0$.

With these new coordinates $(\Phi,\ \theta,\ \phi_0,\ \phi_1)$ and momenta $(\mathcal{N}, \mathcal{M}, \mathcal{M}_0, \mathcal{M}_1)$, we obtain a transformed Hamilton function

$$\begin{aligned}\mathcal{H}' &= \mathcal{H}'(\theta, \phi_0, \phi_1, \mathcal{N}, \mathcal{M}, \mathcal{M}_0, \mathcal{M}_1)\\ &= \Omega_0 \cos(2\phi_0)\sqrt{(\mathcal{N}+\mathcal{M})^2/4 - \mathcal{M}_0^2} + \delta_0\mathcal{M}_0 + \delta_1\mathcal{M}_1\\ &\quad - \Omega_0 \cos(2\phi_1)\sqrt{(\mathcal{N}-\mathcal{M})^2/4 - \mathcal{M}_1^2} + \frac{g}{4}(\mathcal{N}^2 + \mathcal{M}^2 + 2\mathcal{M}_0^2 + 2\mathcal{M}_1^2)\\ &\quad + \frac{\Lambda}{2}\cos(2\theta + \phi_0 - \phi_1)\sqrt{(\mathcal{N}+\mathcal{M}+2\mathcal{M}_0)(\mathcal{N}-\mathcal{M}+2\mathcal{M}_1)}\\ &\quad + \frac{\Lambda}{2}\cos(2\theta - \phi_0 + \phi_1)\sqrt{(\mathcal{N}+\mathcal{M}-2\mathcal{M}_0)(\mathcal{N}-\mathcal{M}-2\mathcal{M}_1)}. \qquad (30)\end{aligned}$$

Obviously, the dynamics conserves the total energy $\mathcal{H}'$ and the total particle number $\mathcal{N}$, as neither time t nor the global phase Φ appears explicitly. However, an interesting feature of this coupled JJ Hamilton function is the negative sign of the Josephson energy in the second line, which leads to a reversal of the current direction and is in direct analogy to equations (2) and (3). The Josephson current relations of the 0–π junction can be obtained from the Hamilton equations for the population change as

$$\dot{\mathcal{M}}_0 = -\frac{\partial\mathcal{H}'}{\partial\phi_0} = \mathcal{I}_0 \sin(2\phi_0) + \mathcal{I}_\mathrm{h}, \qquad (31)$$

$$\dot{\mathcal{M}}_1 = -\frac{\partial\mathcal{H}'}{\partial\phi_1} = -\mathcal{I}_1 \sin(2\phi_1) - \mathcal{I}_\mathrm{h}. \qquad (32)$$

Table 1. Two stationary solutions of the Hamilton equation, energies E_0 and E_1, field amplitudes ($\alpha = (e_0, g_0, e_1, g_1)$ and phases. The global phase of the left site, i.e. $\theta_0 = 0$, was chosen as the common ground.

E	e_0	g_0	e_1	g_1	Φ	ϕ_0	ϕ_1	θ	θ_0	θ_1
−129.84	2.82	−6.48	2.82	6.48	$\frac{\pi}{4}$	$\frac{\pi}{2}$	0	$-\frac{\pi}{4}$	0	$\frac{\pi}{2}$
−117.00	3.16	−6.32	−3.16	−6.32	$-\frac{\pi}{4}$	$\frac{\pi}{2}$	0	$\frac{\pi}{4}$	0	$-\frac{\pi}{2}$

Here, we have introduced critical currents $\mathcal{I}_i$, as well as a hopping current $\mathcal{I}_\mathrm{h}$ by

$$\mathcal{I}_0 = 2\Omega_0\sqrt{(\mathcal{N}+\mathcal{M})^2/4 - \mathcal{M}_0^2} \tag{33}$$

$$\mathcal{I}_1 = 2\Omega_0\sqrt{(\mathcal{N}-\mathcal{M})^2/4 - \mathcal{M}_1^2} \tag{34}$$

$$\begin{aligned}\mathcal{I}_\mathrm{h} = {} & \frac{\Lambda}{2}\sin(2\theta+\phi_0-\phi_1)\sqrt{(\mathcal{N}+\mathcal{M}+2\mathcal{M}_0)(\mathcal{N}-\mathcal{M}+2\mathcal{M}_1)} \\ & -\frac{\Lambda}{2}\sin(2\theta-\phi_0+\phi_1)\sqrt{(\mathcal{N}+\mathcal{M}-2\mathcal{M}_0)(\mathcal{N}-\mathcal{M}-2\mathcal{M}_1)}.\end{aligned} \tag{35}$$

For the parameters $\delta = 1$, $\Omega_0 = 1$, $\Omega_1 = -1$, $\Lambda = 0.1$, $g = 0.005$ and $\mathcal{N} = 100$, we have numerically minimized the energy of equation (21), which is equivalent to the action-angle variable Hamilton function of equation (30) but is more easily accomplished by the method of steepest descent using equation (25). A nonvanishing detuning, δ, was chosen to avoid numerical problems with degeneracies. Consequently, we find two minima with energies $E_0 < E_1$. Please note that the amplitudes of the solutions α are real valued. Due to the invariance of the solutions under global phase change, we can deliberately modify them and choose the global phase of the left site as the common ground $\theta_0 = 0$. In table 1, we have listed the closely spaced energies, the real valued amplitudes and the phases calculated according to equations (27) and (28).

In figure 6, we present the phases for the two states listed in table 1 graphically and compare them with the solution of the sine-Gordon equation [63] already presented in figure 1(b). The gray level represents the value of the Josephson (potential) energy, which is obtained from equations (2) and (3) or equation (30) by keeping the momenta constant and varying the phases θ_i around their equilibrium values. While the solution of the discrete model clearly lacks the smoothness of the continuum model at the 0–π boundary, it represents the asymptotics well. On one hand, this can be rectified by discussing the extended two-component Gross–Pitaevskii equation (13). On the other hand, a few mode quantum model can be very useful for studying the effects of macroscopic tunneling.

4. Conclusion and perspectives

In the present paper, we have briefly summarized the status of fluxon and semifluxon physics in superconductivity. In particular, we have focused on an effect that exists in a long 0–π geometry where two JJs were in the ground state and one obtains a Josephson vortex of fractional magnetic flux, pinned at the 0–π boundary. Depending on the preparation procedure, this ‘classical’ state

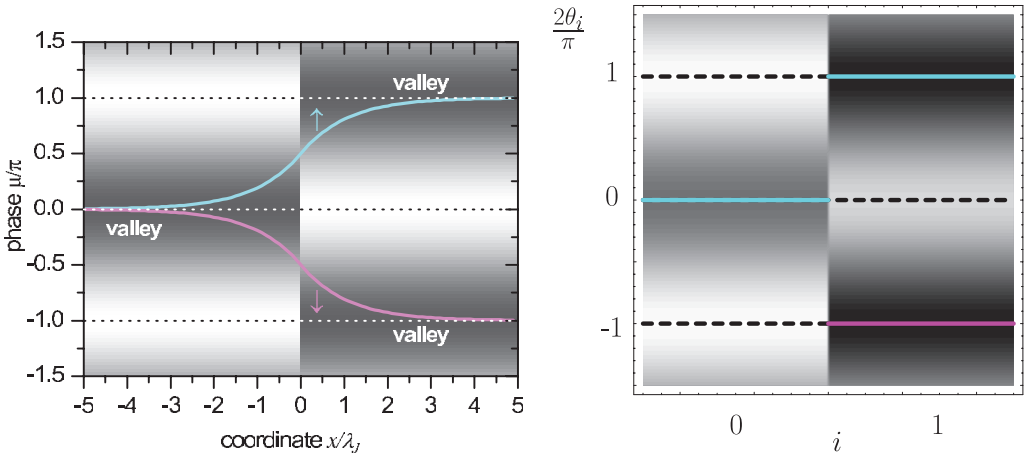

Figure 6. Comparison of a spatially extended 0–π-junction in a superconductor (left panel) calculated according to the sine-Gordon equation [63] to an analog, two-site junction in an atomic BEC (right panel). We have plotted the scaled global phase θ_i versus the site index $i = 0, 1$. The gray level represents the value of the Josephson (potential) energy, where dark means low values and light means high values.

of the superconducting device can occur in two different configurations: with the magnetic flux equal to $+\Phi_0/2$ or $-\Phi_0/2$.

This arrangement of superconducting junctions has been analyzed and transferred to the context of an atomic bosonic quantum gas, where two-state atoms in a double well trap are coupled in a similar fashion. There, the optical 0–π junction is represented by the left/right localized internal atomic JJs and a jumping phase of the complex-valued Rabi frequency. We have derived a simple four-mode model for this case and showed that in the 'classical' approximation it qualitatively resembles the semifluxons seen in superconductivity.

In the superconducting case, one observes a smooth spatial behavior of the phase across the 0–π boundary. In the atomic case, this will emerge also by a more realistic modeling for the Rabi-frequency and spatial motion. This is currently under investigation. Eventually, the four-mode, 0–π Josephson model will also be instrumental in examining the quantum properties of these macroscopic semifluxon states and we will explore the macroscopic tunneling between them [63]. This is also a work in progress and will be reported in a forthcoming publication.

Acknowledgments

The authors acknowledge the support of this work by the Deutsche Forschungsgemeinschaft via the SFB/TRR 21, which is a collaboration of the Universities of Stuttgart, Tübingen and Ulm, as well as the Max-Planck Institute for Solid-State Physics in Stuttgart. RW and WS are also grateful for the support from the Landestiftung Baden-Württemberg (AKZ 0904Atom14) as well as stimulating discussions with K Vogel.

References

[1] Arimondo E, Phillips W D and Strumia F (ed) 1992 *Laser Manipulation of Atoms and Ions* (Amsterdam: North-Holland)
[2] Pitaevskii L and Stringari S 2003 *Bose–Einstein Condensation* (Oxford: Clarendon)
[3] Buckel W and Kleiner R 2004 *Superconductivity: Fundamentals and Applications* 2nd edn (New York: Wiley-VCH)
[4] Folman R, Krüger P, Schmiedmayer J, Denschlag J and Henkel C 2002 Mircoscopic atom optics: from wires to an atom chip *Adv. At. Mol. Opt. Phys.* **48** 263
[5] Fortágh J and Zimmermann C 2007 Magnetic microtraps for ultracold atoms *Rev. Mod. Phys.* **79** 235
[6] Du S *et al* 2004 Atom-chip Bose–Einstein condensation in a portable vacuum cell *Phys. Rev.* A **70** 053606
[7] Vogel A *et al* 2006 Bose–Einstein condensates in microgravity *Appl. Phys.* B **84** 664
[8] Nandi G, Walser R, Kajari E and Schleich W P 2007 Dropping cold quantum gases on earth over long times and large distances *Phys. Rev.* A **76** 63617
[9] Könemann T *et al* 2007 A freely falling magneto-optical trap drop tower experiment *Appl. Phys.* B **89** 431
[10] Likharev K 1979 Superconducting weak links *Rev. Mod. Phys.* **51** 101
[11] Barone A and Paterno G 1982 *Physics and Application of the Josephson Effect* (New York: Wiley Interscience)
[12] Makhlin Y, Schön G and Shnirman A 2001 Quantum-state engineering with Josephson-junction devices *Rev. Mod. Phys.* **73** 357
[13] Castin Y and Dalibard J 1997 Relative phase of two Bose–Einstein condensates *Phys. Rev.* A **55** 4330
[14] Andrews M, Townsend C, Miesner H J, Durfee D, Kurn D and Ketterle W 1997 Observation of interference between two Bose condensates *Science* **275** 637
[15] Ketterle W, Durfee D and Stamper-Kurn D 1999 Making, probing and understanding Bose–Einstein condensates *Proc. Int. School of Physics 'Enrico Fermi', Course CXL. Soc. Italiana di Fisica, Bologna, Italy* ed M Inguscio, S Stringari and C Wieman (Amsterdam: IOS Press)
[16] Anderson B P and Kasevich M A 1998 Macroscopic quantum interference from atomic tunnel arrays *Science* **282** 1686
[17] Zapata I, Sols F and Leggett T 1998 Josephson effect between trapped Bose–Einstein condensates *Phys. Rev.* A **57** R28
[18] Williams J, Walser R, Cooper J, Cornell E and Holland M 1999 Nonlinear Josephson-type oscillations of a driven two-component Bose–Einstein condensate *Phys. Rev.* A **59** 31
[19] Williams J, Walser R, Cooper J, Cornell E and Holland M 2000 Excitation of a dipole topological state in a strongly coupled two-component Bose–Einstein condensate *Phys. Rev.* A **61** 033612
[20] Leggett A 2001 Bose–Einstein condensation in the alkali gases: some fundamental concepts *Rev. Mod. Phys.* **73** 307
[21] Giovanazzi S, Smerzi A and Fantoni S 2000 Josephson effects in dilute Bose–Einstein condensates *Phys. Rev. Lett.* **84** 4521
[22] Sakellari E, Proukakis N, Leadbeater M and Adams C 2004 Josephson tunneling of a phase imprinted Bose–Einstein condensate in a time-dependent condensate *New J. Phys.* **6** 42
[23] Albiez M, Gati R, Fölling J, Hunsmann S, Cristian M and Oberthaler M K 2005 Direct observation of tunneling and nonlinear self-trapping in a single bosonic Josephson junction *Phys. Rev. Lett.* **95** 010402
[24] Gati R and Oberthaler M 2007 A bosonic Josephson junction *J. Phys. B: At. Mol. Opt. Phys.* **40** R61
[25] Cataliotti F *et al* 2001 Josephson junction arrays with Bose–Einstein condensates *Science* **293** 843
[26] Nandi G, Sizman A, Fortágh J and Walser R 2007 A numberfilter for matterwaves *Preprint* 0710.1737
[27] Kulic M 2007 π-superconducting quantum interference device from ultracold fermionic gases *Phys. Rev.* A **76** 53625
[28] Bloch I 2005 Ultracold quantum gases in optical lattices *Nat. Phys.* **1** 23
[29] Fölling S *et al* 2007 Direct observation of second-order atom tunnelling *Nature* **448** 1029

[30] Hadzibabic Z, Stock S, Battelier B, Bretin V and Dalibard J 2004 Interference of an array of independent Bose–Einstein condensates *Phys. Rev. Lett.* **93** 180403
[31] Kaurov V M and Kuklov A B 2006 Atomic Josephson vortices *Phys. Rev.* A **73** 013627
[32] Kaurov V M and Kuklov A B 2005 Josephson vortex between two atomic Bose–Einstein condensates *Phys. Rev.* A **71** 011601
[33] Goldobin E, Koelle D and Kleiner R 2002 Semifluxons in long Josephson 0–π-junctions *Phys. Rev.* B **66** 100508
[34] Kleiner R, Steinmeyer F, Kunkel G and Müller P 1992 Intrinsic Josephson effects in $Bi_2Sr_2CaCu_2O_8$ single crystals *Phys. Rev. Lett.* **68** 2394–7
[35] Kleiner R and Müller P 1994 Intrinsic Josephson effects in high-T_c superconductors *Phys. Rev.* B **49** 1327–41
[36] Ryazanov V V, Oboznov V A, Rusanov A Y, Veretennikov A V, Golubov A A and Aarts J 2001 Coupling of two superconductors through a ferromagnet: evidence for a π junction *Phys. Rev. Lett.* **86** 2427
[37] Blum Y, Tsukernik A, Karpovski M and Palevski A 2002 Oscillations of the superconducting critical current in Nb–Cu–Ni–Cu–Nb junctions *Phys. Rev. Lett.* **89** 187004
[38] Bauer A *et al* 2004 Spontaneous supercurrent induced by ferromagnetic π junctions *Phys. Rev. Lett.* **92** 217001
[39] Sellier H, Baraduc C, Lefloch F and Calemczuk R 2004 Half-integer Shapiro steps at the 0–π crossover of a ferromagnetic Josephson junction *Phys. Rev. Lett.* **92** 257005
[40] Oboznov V A, Bol'ginov V V, Feofanov A K, Ryazanov V V and Buzdin A I 2006 Thickness dependence of the Josephson ground states of superconductor–ferromagnet–superconductor junctions *Phys. Rev. Lett.* **96** 197003
[41] Kontos T, Aprili M, Lesueur J, Genêt F, Stephanidis B and Boursier R 2002 Josephson junction through a thin ferromagnetic layer: negative coupling *Phys. Rev. Lett.* **89** 137007
[42] Weides M *et al* 2006 High quality ferromagnetic 0 and π Josephson tunnel junctions *Appl. Phys. Lett.* **89** 122511
[43] Vavra O *et al* 2006 0 and π phase Josephson coupling through an insulating barrier with magnetic impurities *Phys. Rev.* B **74** 020502
[44] Cleuziou J P, Wernsdorfer W, Bouchiat V, Ondarcuhu T and Monthioux M 2006 Carbon nanotube superconducting quantum interference device *Nat. Nanotechnol.* **1** 53–9
[45] van Dam J A, Nazarov Y V, Bakkers E P A M, De Franceschi S and Kouwenhoven L P 2006 Supercurrent reversal in quantum dots *Nature* **442** 667–70
[46] Bulaevskiĭ L N, Kuziĭ V V and Sobyanin A A 1977 *Pis. Zh. Eksp. Teor. Fiz.* **25** 314
Bulaevskiĭ L N, Kuziĭ V V and Sobyanin A A 1977 Superconducting system with weak coupling to the current in the ground state *JETP Lett.* **25** 290–4 (Engl. Transl.)
[47] Bulaevskii L N, Kuzii V V and Sobyanin A A 1978 On possibility of the spontaneous magnetic flux in a Josephson junction containing magnetic impurities *Solid State Commun.* **25** 1053–7
[48] Xu J H, Miller J H and Ting C S 1995 π-vortex state in a long 0–π-Josephson junction *Phys. Rev.* B **51** 11958
[49] Kirtley J R, Tsuei C C and Moler K A 1999 Temperature dependence of the half-integer magnetic flux quantum *Science* **285** 1373
[50] Kirtley J R *et al* 1996 Direct imaging of integer and half-integer Josephson vortices in high-T_c grain boundaries *Phys. Rev. Lett.* **76** 1336
[51] Smilde H J H, Ariando, Blank D H A, Gerritsma G J, Hilgenkamp H and Rogalla H 2002 *d*-Wave-induced Josephson current counterflow in $YBa_2Cu_3O_7$/Nb zigzag junctions *Phys. Rev. Lett.* **88** 057004
[52] Ariando *et al* 2005 Phase-sensitive order parameter symmetry test experiments utilizing $Nd_{2-x}Ce_xCuO_{4-y}$/Nb zigzag junctions *Phys. Rev. Lett.* **94** 167001
[53] Hilgenkamp H *et al* 2003 Ordering and manipulation of the magnetic moments in large-scale superconducting π-loop arrays *Nature* **422** 50–3
[54] Kirtley J R, Tsuei C C, Ariando, Smilde H J H and Hilgenkamp H 2005 Antiferromagnetic ordering in arrays of superconducting π-rings *Phys. Rev.* B **72** 214521

[55] Kogan V G, Clem J R and Kirtley J R 2000 Josephson vortices at tricrystal boundaries *Phys. Rev.* B **61** 9122–9
[56] Zenchuk A and Goldobin E 2004 Analytical analysis of ground states of 0–π long Josephson junctions *Phys. Rev.* B **69** 024515
[57] Susanto H, van Gils S A, Visser T P P, Ariando, Smilde H J H and Hilgenkamp H 2003 Static semifluxons in a long Josephson junction with π-discontinuity points *Phys. Rev.* B **68** 104501
[58] Kirtley J R, Moler K A and Scalapino D J 1997 Spontaneous flux and magnetic-interference patterns in 0–π Josephson junctions *Phys. Rev.* B **56** 886
[59] Goldobin E, Stefanakis N, Koelle D and Kleiner R 2004 Fluxon–semifluxon interaction in an annular long Josephson 0–π junction *Phys. Rev.* B **70** 094520
[60] Lazarides N 2004 Critical current and fluxon dynamics in overdamped 0–π Josephson junctions *Phys. Rev.* B **69** 212501
[61] Goldobin E, Koelle D and Kleiner R 2003 Ground state and bias current induced rearrangement of semifluxons in 0–π-Josephson junctions *Phys. Rev.* B **67** 224515
[62] Susanto H, Goldobin E, Koelle D, Kleiner R and van Gils S A 2005 Controllable plasma energy bands in a one-dimensional crystal of fractional Josephson vortices *Phys. Rev.* B **71** 174510
[63] Goldobin E *et al* 2005 Quantum tunneling of semifluxons in a 0–π–0 long Josephson junction *Phys. Rev.* B **72** 054527
[64] Schleich W P 2001 *Quantum Optics in Phase Space* (Berlin: Wiley-VCH)
[65] Feynman R P and Hibbs A H 1965 *Quantum Mechanics and Path Integrals* (New York: McGraw-Hill)
[66] Kohn W 1959 Analytic properties of Bloch waves and Wannier functions *Phys. Rev.* **115** 809
[67] Jaksch D, Bruder C, Cirac J, Gardiner C and Zoller P 1998 Cold bosonic atoms in optical lattices *Phys. Rev. Lett.* **81** 3108